

NOTES AND CORRESPONDENCE

Temporal Variability of the Large-Scale Geostrophic Surface Velocity in the Northeast Pacific*

P. VAN MEURS

Pacific Marine Environmental Laboratory, Seattle, Washington

P. P. NIILER

Scripps Institution of Oceanography, La Jolla, California

31 December 1995 and 11 March 1996

ABSTRACT

Data from Argos-tracked mixed layer drifters in fall and winter 1987 (49 drifters) and 1989 (16 drifters) are used to investigate the differences in the large-scale surface velocity and eddy activity in the northeast Pacific. The velocities were corrected for wind-induced slippage and corrected for wind-driven (Ekman) flow by matching an Ekman model to the observed currents. The model, which explains 15%–30% of the variance, indicates that the currents are at 60° to the right of the wind. The magnitude of the currents is 30% of the magnitude of the wind stress. In 1987–88, the geostrophic motion in the region from 46.5° to 48.5°N , 142° to 133°W was characterized by an eastward flow of $0.9 (\pm 0.4) \text{ cm s}^{-1}$ and a northward flow of $0.7 (\pm 0.4) \text{ cm s}^{-1}$. In 1989–90, for the same region, the geostrophic eastward component was $3.8 (\pm 0.5) \text{ cm s}^{-1}$, more than four times as large as in 1987–88, and the northward component was $0.3 (\pm 0.5) \text{ cm s}^{-1}$. In this region ageostrophic contributions to the velocities are small.

In 1987–88 the drifter tracks reveal evidence of the presence of several persistent, warm core mesoscale eddies. In 1989–90 there is no evidence of any significant eddy activity. The mean speed of the drifters in 1987–88 was $7.0 (\pm 0.3) \text{ cm s}^{-1}$ and in 1989–90 was $6.5 (\pm 0.4) \text{ cm s}^{-1}$. So, although the average speed is the same, drifters in 1987–88 take a longer time to travel eastward because of the significant north–south excursions due to the mesoscale eddies. Data from two drifter experiments have shown that the variability of mesoscale eddies can result in large interannual differences in estimates of mean velocity.

1. Introduction

The northeast Pacific is characterized by low mean and eddy kinetic energy with most of the energy related to mesoscale eddy features. Paduan and Niiler (1993) found that in the eastern Pacific the eddy energy exceeds the mean kinetic energy by a factor of 4–14. Sverdrup et al. (1942) identified two eastward flowing currents in the interior region of the eastern Pacific: the subarctic current located at about 45°N is part of the Alaskan subarctic gyre and the North Pacific Current located at about 37°N is part of the North Pacific subtropical gyre. Data collected at Ocean Station Papa at 50°N , 145°W show significant year to year variability (Tabata 1965).

Reid and Arthur (1975) and Wyrtki (1975) show dynamic topography charts of this region indicating the presence of the two-gyre system. Historical ship drift data indicate a slow eastward flow in the area separating the Alaskan subarctic gyre from the North Pacific subtropical gyre (Wakata and Sugimori 1990) and (Meehl 1982). These estimates of surface currents are strongly wind driven, as they are based on ship drift observations. Kirwan et al. (1978), McNally (1981), and McNally and White (1985) used drifters to measure the surface and near-surface currents in the eastern midlatitude Pacific. Figure 1 of Kirwan et al. (1978) and McNally (1981) shows an eastward flow and a bifurcation of the flow with drifters released north of the Subarctic Front getting caught in the northward flowing Alaskan Current and those released south of the Subarctic Front following the southward flowing eastern boundary current of the subtropical gyre. Our data (Fig. 1) reveal similar bifurcation of the flow in 1987, while in 1989 there is less evidence of this bifurcation (Fig. 2). Unlike our findings in 1987 (Fig. 1), McNally (1981) shows little eddy activity, similar to the HEAVY 89 experiment (Fig.

*NOAA Pacific Marine Environmental Laboratory Contribution Number 1749.

Corresponding author address: Dr. Pim van Meurs, NOAA/PMEL/R/E/PM, BIN C15700/Bldg. 3, 7600 Sand Point Way NE, Seattle, WA 98115-0070.
E-mail: pim@pmel.noaa.gov

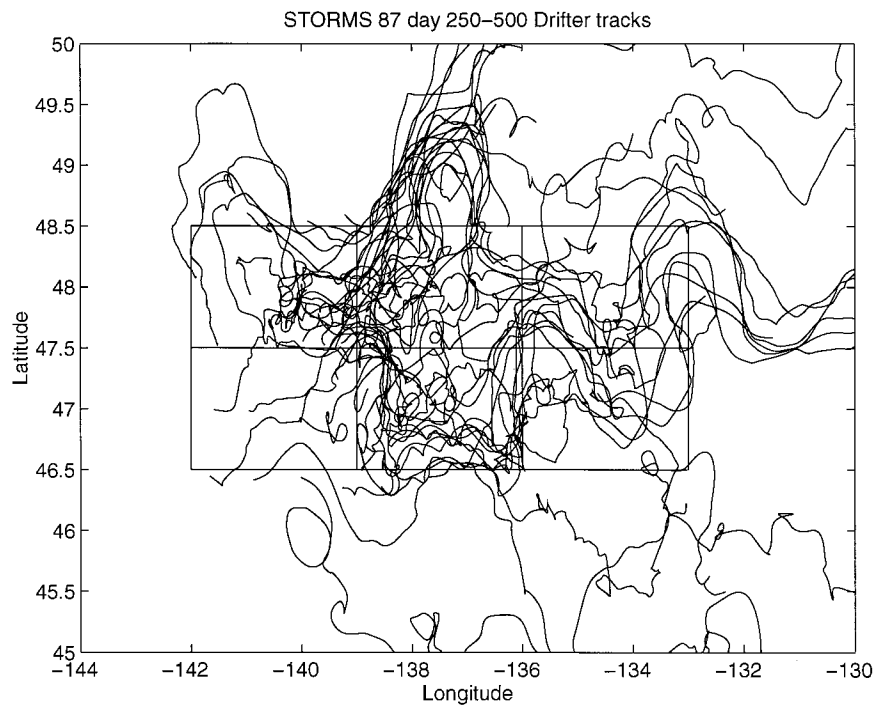


FIG. 1. Filtered drifter tracks for the STORMS 87 experiment for days 250-500, 1987. Regions 1-3 start at the bottom left corner, regions 4-6 start at the top left corner.

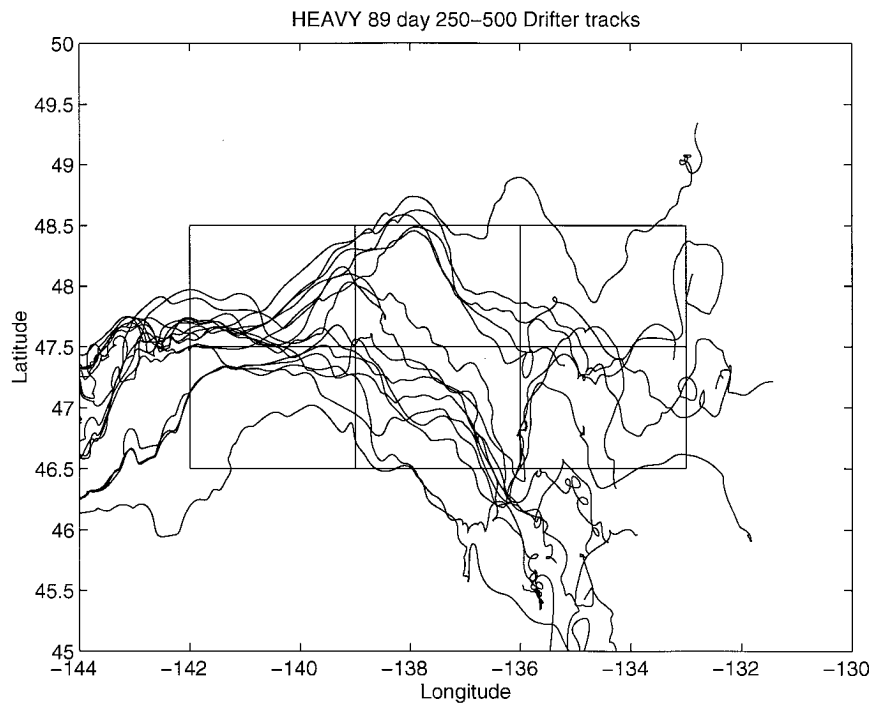


FIG. 2. Filtered drifter tracks for the HEAVY 89 experiment for days 250-500, 1989. Regions 1-3 start at the bottom left corner, regions 4-6 start at the top left corner.

TABLE 1. Estimates of time and length scales and single particle diffusivities based on Lagrangian autocorrelation functions. PN93 refers to Paduan and Niiler (1993).

| Experiment | Timescale (days) | | Length scale (km) | | Diffusivity ($\text{m}^2 \text{s}^{-1}$) | |
|------------|------------------|---------------|-------------------|----------------|--|----------------|
| | Zonal | Meridional | Zonal | Meridional | Zonal | Meridional |
| STORMS 87 | 2.7 ± 0.5 | 3.3 ± 0.5 | 12.2 ± 2.5 | 16.2 ± 2.7 | 655 ± 155 | 925 ± 175 |
| HEAVY 89 | 2.9 ± 1.3 | 3.7 ± 0.8 | 11.2 ± 5.3 | 17.3 ± 4.3 | 505 ± 256 | 957 ± 272 |
| PN93 | 2.8 ± 0.7 | 3.8 ± 0.4 | 13.9 ± 4.1 | 22.0 ± 3.1 | 835 ± 299 | 1524 ± 332 |

2). McNally (1981) found average drogued buoy speeds of $7 (\pm 4) \text{ cm s}^{-1}$ for October and November $9 (\pm 2) \text{ cm s}^{-1}$ for December and January, and $16 (\pm 5) \text{ cm s}^{-1}$ for February–March, and in April the average speed dropped to $8 (\pm 4) \text{ cm s}^{-1}$ (Fig. 2 and Table 1), indicating a large seasonal variability. The currents were at an angle of about 30° to the right of the surface wind with speeds of about 1.5% of the wind speed. The water-following capabilities of mixed layer drifters is to a large extent determined by the ratio (R) of the drag of the drogue area to the drag of the submerged float and tether. The drifters used by McNally had either a window-shade or parachute drogue attached at 30-m depth. The window-shade drogues had a drag area ratio R of 10–12 and the parachute drogues had a drag ration of about 50–70, similar to the ones used in this study. However, the parachute drogues are prone to collapsing, reducing the drag ratio significantly. This might explain why McNally found similar results for drogued and undrogued drifters. Niiler and Paduan (1995) used data from the STORMS 87 and HEAVY 89 experiment and found that the currents are at an angle of 68° to the right of the wind with speeds of 0.5% of the wind speed. Their model explains 20%–40% of the variance. They, however, did not address the spatial and temporal variabilities. We will show that increased eddy activity during the STORMS 87 experiment effectively reduced the mean east–west velocity.

2. The data

Three different drifter designs were used in the experiments: holey-sock, MINISTAR, and TRISTAR-II drifters (Niiler and Paduan 1995; Niiler et al. 1995). Typically 8–10 fixes per day were received by the ARGOS satellites with 70% of the intervals between fixes at 3 hours or less. In the Ocean Storms experiment in October 1987 (STORMS 87) a group of 49 TRISTAR-II mixed layer drifters (all drogued at 15 m) were released in an area centered at 46.5°N , 137.5°W . Paduan and Niiler (1993) have summarized these data, showing a well-determined eastward flow of 4.4 cm s^{-1} through a field of somewhat discrete warm-core eddies. In October 1989, 16 drifters (8 holey-sock and 8 MINISTAR drifters) were released in a test of the effects of heavy weather on drifter survival (WOCE HEAVY 89). While these also moved eastward, significant differences were noted in their motion.

The region of study, a rectangular square in the north-east Pacific limited by 46.5° and 48.5°N and 142° to 133°W , was chosen because there was adequate drifter coverage of this area in both years (Fig. 1 and 2). The area was further divided into six subregions to study the spatial differences. Significantly less eddy activity was observed in 1989 (Fig. 2) than in 1987 (Fig. 1), so we were curious if the mean velocities averaged over the six $1^\circ (\text{lat}) \times 3^\circ (\text{long})$ areas would also differ.

Figure 3 shows the distribution over time of drifter observations in the six regions for the STORMS 87 experiment for days 250–500. Figure 4 shows the distribution for the HEAVY 89 experiment for days 330–530. The time frames were chosen to maximize drifter coverage. The figures reveal that the HEAVY 89 observations tend to be about 10 weeks later than the STORMS 87 observations for regions 1, 2, 3, and 4. Regions 5 and 6 show more overlap in time. Thus, a direct comparison in time and space between 1987 and 1989 is complicated. However, since we correct for wind-slip and wind-driven flow, the seasonal differences in direct wind forcing have been eliminated as a source. A likely remaining candidate are variations in eddy activity in the region.

The drifter position data obtained from the ARGOS satellites were 1) linearly interpolated to 0.25 days, 2) time differenced to obtain velocity estimates, 3) filtered with a Butterworth filter with a cutoff frequency of 0.35 days^{-1} , and 4) corrected for wind-induced slippage of the drogues by using ECMWF (European Centre for Medium-Range Weather Forecasts) 6-h winds, which were interpolated to the drifter's position (Niiler et al. 1995). The wind velocity and stress data were filtered with the same Butterworth filter and 5) corrected for wind-induced drift (Ekman) by using a linear Ekman balance model that relates the Ekman currents to the local wind stress (Niiler and Paduan 1995).

Argos derived positions have an error of typically 300 m, which translates to velocity errors of less than 0.4 cm s^{-1} for observations separated in time by one day.

The filter is used to remove the significant energy in the inertial band as well as to limit the analysis to the frequency band for which a significant correlation between the wind and the currents was found (Niiler and Paduan 1995). To eliminate phase errors the data were filtered in a forward and reverse direction, this procedure results in a zero-phase distortion and doubles the filter order.

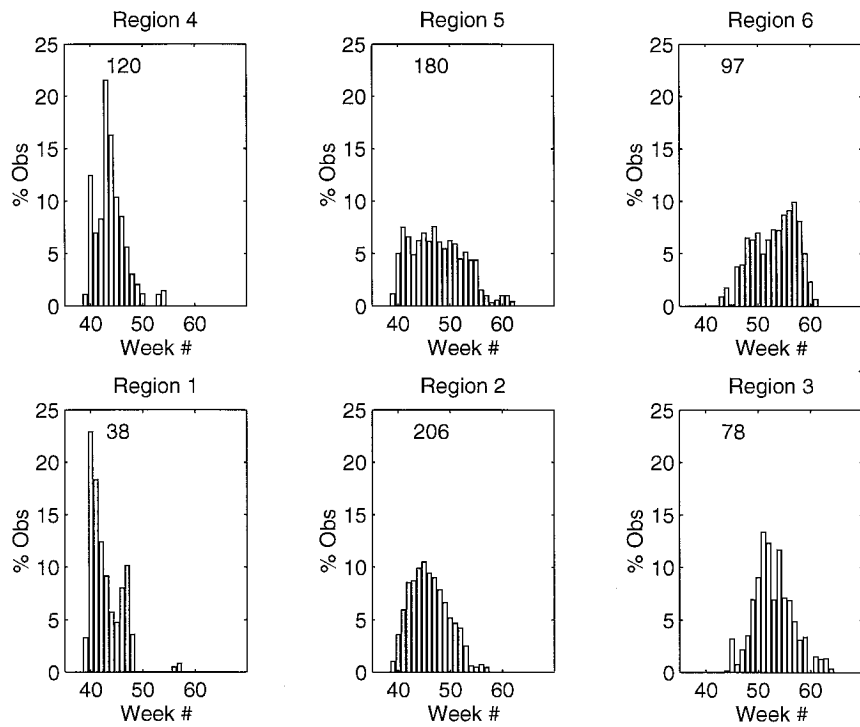


FIG. 3. Distribution of independent drifter observation for STORMS 87 as function of time for the six regions.

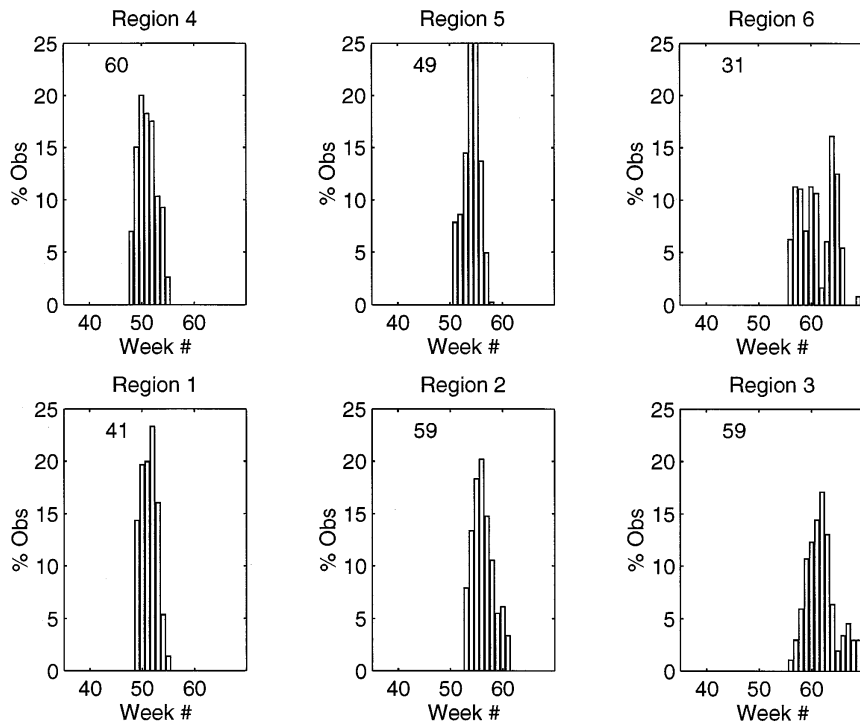


FIG. 4. Distribution of independent drifter observation for HEAVY 89 as function of time for the six regions.

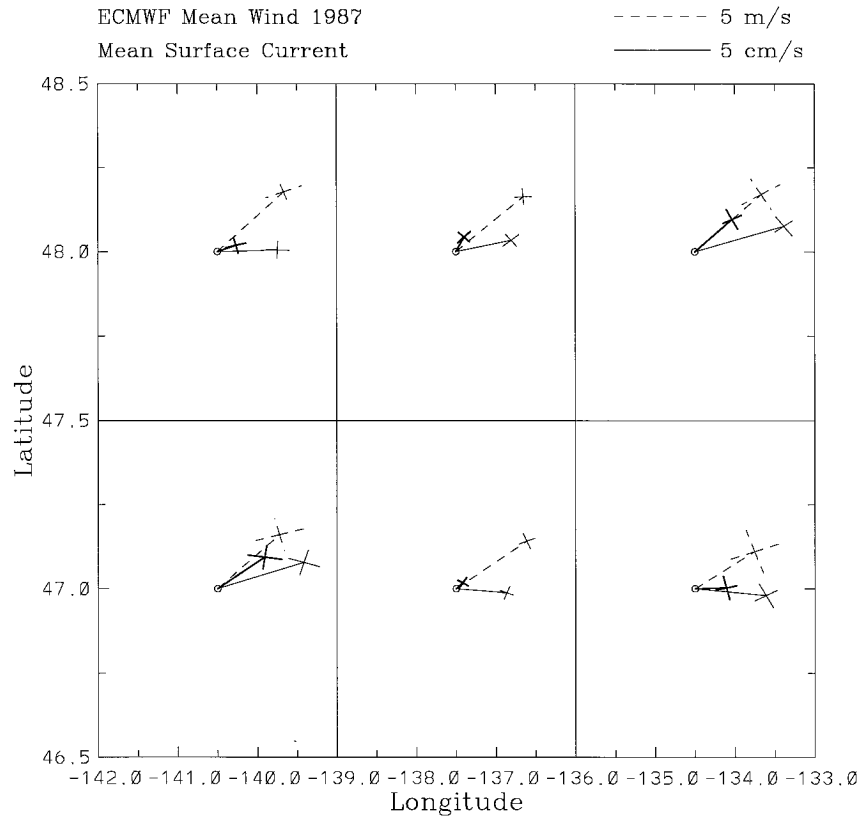


FIG. 5. Mean ECMWF wind speeds (dashed), slip corrected mean currents (light solid), and Ekman model corrected mean currents (dark solid) for STORMS 87 (October 1987 until March 1988). Crosses at the end of the vector indicate the 95% error bounds in the direction of the minor and major axes of the variance tensor assuming a 4-day timescale for independent observations.

Niiler et al. (1995) measured the slippage of drogues through the water that is caused by wind by attaching current meters to the drogue. Their model included wind speed and velocity shear across the drogue. Since we only have wind measurements, we repeated their analysis using the following model:

$$U_s = \frac{a}{R} U_w. \quad (1)$$

With $U_s = (u_s, v_s)$ the wind slippage vector (in cm s^{-1}) in the direction of the wind velocity vector $U_w = (u_w, v_w)$ (in m s^{-1}). Here $a = 7.0 \pm 0.7$ is obtained from a least square fit of measured slip and wind speed and R is the drag area ratio of the drifter involved. The drag area ratio was 77 for the TRISTAR-II drifters and 49 for the holey-sock and MINISTAR drifters. The model explained 66% of the variance. Niiler and Paduan (1995) used a similar model, which accounted for 45% of the variance with $a = 7.0$. All error bounds are the 95% error limits given by 1.96σ . ECMWF winds are available every 6 hours on a 1.2° latitude/longitude grid.

a. STORMS 87

The STORMS 87 experiment has been described extensively in Paduan and Niiler (1993) but some aspects

of it will be repeated here. The STORMS 87 upper-ocean data is from 49 closely spaced drifters. Figure 1 shows the drifter tracks for days 250–500 as well as the region and subregions of this study and shows the presence of several eddies and a generally eastward motion of the drifters.

Figure 5 shows the average wind vector (dashed line) and slip-corrected mean velocity (light solid line) for days 250–450 (October 1987 to March 1988). The cross at the end of the vectors are the 95% confidence intervals (1.96σ) for the velocity vector in the directions of the major and minor axis of the variance ellipse. The mean wind is consistently in a northeastward direction, with most variability closer to the coast (regions 3 and 6). The mean current is eastward, but as the coast is approached it deflects to the north in region 6 and to the south in region 3.

b. HEAVY 89

In 1989 during the HEAVY 89 experiment, 16 drifters were deployed in four groups of 4 drifters of different design, 2 holey-sock drifters, and 2 MINISTAR drifters. The drifters were deployed on a north–south line along 145°W . The drifters tend to stay together for quite a

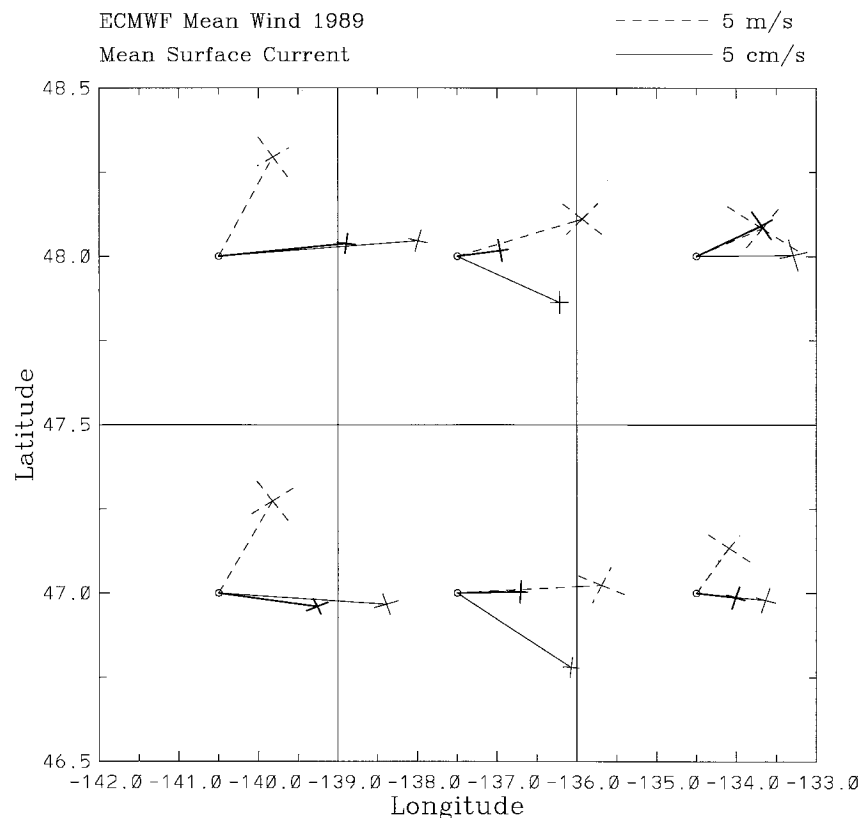


FIG. 6. As in Fig. 5 but for HEAVY 89 (December 1987 until May 1988).

long time, effectively decreasing the longitudinal coverage of the area (Fig. 2). The tracks show no substantial sign of eddy activity but do show a persistent south-eastward flow in regions 2 and 5. Since the drifters are deployed west of the area of interest, it takes about two months for the drifters to reach the area and the data analyzed last from day 330 to 530 (December 1989 to May 1990).

Figure 6 shows the average wind vector (dashed line) and the slip-corrected mean currents (light solid line) for each of the six regions. The wind speed is higher in the western boxes (1, 2, 4, 5) and decreases toward the east. The tracks (Fig. 2) show a persistent southward motion of the drifters in boxes 2 and 5 where the wind is eastward. The winds during HEAVY 89 are stronger than during STORMS 87 and while during STORMS 87 the winds have a very similar direction, winds during HEAVY 89 in regions 2 and 5 have a more eastward direction than in other subregions. Anomalous sea level pressure maps show in the time period November 1989–January 1990 the presence of anomalous pressure over the northeast Pacific, generating the persistent south-eastward winds (NOAA, Climate Diagnostic Bulletin 1989–90).

3. Single particle statistics

To determine the decorrelation timescales of the velocities we calculated the sample Lagrangian autocor-

relation function and calculated Lagrangian time and length scales (Paduan and Niiler 1993). The Lagrangian integral time and length scales are summarized in Table 1. The data used are from all drifters with data between day 250 and day 500 for the total region from 46.5° to 48.5°N, 142° to 133°W. From this table it is evident that 4 days is a reasonable estimate for the independence timescale for the velocity dataset. The independence timescale allows us to obtain estimates for the 95% error bounds of the mean for the average velocities derived for each subregion. Although the zonal timescales were smaller than meridional timescales, it is only marginally significant at 95%. Paduan and Niiler (1993) found larger values for the length scales and diffusivity. This is because they included several eddies outside our region of study (for instance, the eddy at 51°N, 135°W). Furthermore, 2 drifters that went north into the Alaskan Current were not included in our study.

4. Circulation statistics

a. STORMS 87

Table 2 shows the number of independent observations estimated using an independence timescale of 4 days, the mean zonal and meridional velocity, and their variance and mean and eddy kinetic energy for the six subregions during the STORMS 87 experiment. The first

TABLE 2. Number of independent observations (Obs), based on a 4-day independence timescale; mean velocity and standard error, variance and mean and eddy kinetic energy for the six regions, the total region, and for Paduan and Niiler (1993) for slip corrected and Ekman model corrected velocity dataset for STORMS 87 for the period October 1987–March 1988. PN93 refers to Paduan and Niiler (1993).

| Region | Obs | Mean velocity (cm s ⁻¹) | | Variance (cm ² s ⁻²) | | Kinetic energy (cm ² s ⁻²) | |
|--------|----------|-------------------------------------|------------|---|-------------------|---|------|
| | <i>N</i> | \bar{u} | \bar{v} | $\overline{u'^2}$ | $\overline{v'^2}$ | MKE | EKE |
| 1 | 38 | 4.5 ± 1.7 | 1.6 ± 1.5 | 28.3 | 23.6 | 11.4 | 25.6 |
| | | 2.5 ± 1.8 | 1.9 ± 1.4 | 32.0 | 19.7 | 4.8 | 25.2 |
| 2 | 206 | 2.6 ± 0.7 | -0.2 ± 0.8 | 30.2 | 33.6 | 3.5 | 31.8 |
| | | 0.3 ± 0.7 | 0.3 ± 0.7 | 24.1 | 27.4 | 0.1 | 25.6 |
| 3 | 78 | 3.7 ± 1.4 | -0.4 ± 1.5 | 38.4 | 45.5 | 6.9 | 41.7 |
| | | 1.6 ± 1.1 | 0.1 ± 1.4 | 25.3 | 39.8 | 1.3 | 32.4 |
| 4 | 119 | 3.1 ± 1.2 | 0.1 ± 1.0 | 43.3 | 33.2 | 5.0 | 38.0 |
| | | 1.0 ± 1.1 | 0.4 ± 1.0 | 37.7 | 30.2 | 0.5 | 33.3 |
| 5 | 179 | 2.9 ± 1.0 | 0.7 ± 1.0 | 46.6 | 43.2 | 4.4 | 44.8 |
| | | 0.4 ± 0.9 | 0.9 ± 0.9 | 37.2 | 37.6 | 0.5 | 37.3 |
| 6 | 96 | 4.6 ± 1.2 | 1.5 ± 1.3 | 37.5 | 42.7 | 12.0 | 40.0 |
| | | 1.9 ± 1.1 | 1.9 ± 1.3 | 31.9 | 40.2 | 3.7 | 35.9 |
| All | 717 | 3.3 ± 0.5 | 0.4 ± 0.5 | 38.8 | 38.4 | 5.4 | 38.5 |
| PN93 | 522 | 0.9 ± 0.4 | 0.7 ± 0.4 | 31.8 | 33.5 | 0.7 | 32.6 |
| | | 4.4 ± 0.5 | 0.7 ± 0.6 | 47.0 | 34.0 | 10.0 | 40.0 |

row for the mean velocity, variance, and energy boxes contains the slip corrected numbers and the second row shows the slip- and Ekman-model corrected velocities.

The mean east–west velocity, using data from all six regions, $\bar{u} = 3.3 (\pm 0.5)$ cm s⁻¹ is much larger than the mean north–south velocity $\bar{v} = 0.4 (\pm 0.5)$ cm s⁻¹. This is to be expected in this region between the North Pacific subtropical gyre and the Alaskan subarctic gyre. It should also be noted that the east–west and north–south variances in almost all regions are of similar magnitude. We find an average eddy kinetic energy (EKE) of 38.5 cm² s⁻² and an average mean kinetic energy (MKE) of 5.4 cm² s⁻². Paduan and Niiler (1993) computed a larger east–west velocity of $\bar{u} = 4.4 (\pm 0.5)$ cm s⁻¹, but the north–south velocity of $\bar{v} = 0.7 (\pm 0.6)$ cm s⁻¹ was

identical to our computations. They also found a significantly higher north–south variance of 47.0 cm² s⁻² and an almost identical east–west variance of 34.0 cm² s⁻². The eddy kinetic energy has a similar value of 40.0 cm² s⁻². The difference can be explained by the fact that they included an energetic eddy located at 135°W and 51°N. This eddy (loop III in their paper) has an average speed of 20.2 (±4.1) cm s⁻¹ adding significantly to the east–west velocity as well as the eddy kinetic energy.

b. HEAVY 89

Table 3 shows the statistics for the 1989 Heavy Weather dataset. The number of independent observa-

TABLE 3. Number of independent observations based on a 4-day independence timescale, mean velocity and standard error, variance and mean and eddy kinetic energy for the six regions, the total region for the slip corrected and Ekman model corrected velocity set for HEAVY 89 for December 1989–May 1990.

| Region | Obs | Mean velocity (cm s ⁻¹) | | Variance (cm ² s ⁻²) | | Kinetic energy (cm ² s ⁻²) | |
|--------|----------|-------------------------------------|------------|---|-------------------|---|------|
| | <i>N</i> | \bar{u} | \bar{v} | $\overline{u'^2}$ | $\overline{v'^2}$ | MKE | EKE |
| 1 | 41 | 8.8 ± 1.3 | -0.7 ± 1.2 | 17.9 | 16.1 | 38.8 | 16.9 |
| | | 5.2 ± 1.2 | -0.8 ± 1.0 | 14.7 | 11.1 | 13.6 | 12.8 |
| 2 | 59 | 6.0 ± 0.8 | -4.4 ± 1.2 | 10.9 | 22.0 | 27.5 | 16.4 |
| | | 3.3 ± 0.7 | 0.1 ± 1.3 | 7.6 | 25.2 | 5.5 | 16.3 |
| 3 | 58 | 3.6 ± 1.1 | -0.4 ± 1.5 | 18.3 | 33.0 | 6.6 | 25.6 |
| | | 2.1 ± 1.0 | -0.3 ± 1.3 | 16.1 | 26.8 | 2.1 | 21.4 |
| 4 | 59 | 10.4 ± 1.0 | 0.9 ± 1.3 | 16.5 | 25.4 | 55.0 | 20.9 |
| | | 6.7 ± 1.0 | 0.8 ± 1.2 | 13.9 | 20.8 | 22.7 | 17.3 |
| 5 | 49 | 5.3 ± 0.9 | -2.7 ± 1.3 | 11.3 | 21.7 | 18.1 | 16.4 |
| | | 2.2 ± 0.9 | 0.3 ± 1.3 | 9.5 | 21.6 | 2.6 | 15.5 |
| 6 | 31 | 5.1 ± 1.5 | 0.1 ± 1.9 | 17.4 | 29.5 | 12.8 | 23.3 |
| | | 3.4 ± 1.5 | 1.8 ± 1.8 | 17.8 | 24.9 | 7.4 | 21.2 |
| All | 299 | 6.6 ± 0.5 | -1.3 ± 0.6 | 21.1 | 28.4 | 22.6 | 24.8 |
| | | 3.8 ± 0.5 | 0.3 ± 0.5 | 15.9 | 22.6 | 7.4 | 19.2 |

tions is a factor of 2–4 smaller than for the STORMS 87 dataset, which explains the larger 95% error bounds for the velocity components. Nevertheless, the east–west velocity $\bar{u} = 6.6 (\pm 0.5) \text{ cm s}^{-1}$ is significantly larger (by a factor of 2) than the east–west velocity in the STORMS 87 experiment. We note that the east–west velocity is much larger than the north–south velocity and that the spatial variability of the mean velocity is much larger than in the STORMS 87 experiment. The east–west variance ($21.1 \text{ cm}^2 \text{ s}^{-2}$) is smaller than the north–south variance ($28.4 \text{ cm}^2 \text{ s}^{-2}$). We observe an eastward decay of east–west velocity in both regions 1–3 and regions 4–6 and a southeastward flow in regions 2 and 5.

Comparison of Fig. 6 with Fig. 5 shows that the currents in 1989 are much stronger and that those in regions 2 and 5 are more southeastward. Since the winds in this region and period show an anomalous east-southeastward flow, we use the local wind to remove the wind-induced slip and the wind-driven part of the flow. The procedure to remove the wind-induced slip has already been discussed in the data section.

5. Local wind-driven currents

In an effort to account for the local wind-driven part of the velocity we used an Ekman–regression model of the wind-driven current, representing the velocity as a complex number (Niiler and Paduan 1995);

$$u + iv = \beta e^{i\theta} \rho_a c_d |u_w + iv_w| (u_w + iv_w) \quad (2)$$

$$u + iv = \beta e^{i\theta} (\tau_x + i\tau_y), \quad (3)$$

where ρ_a is the density of air (1.2 kg m^{-3}), c_d is the drag coefficient (1.2×10^{-3}), β is the amplitude relating Ekman currents to the wind stress, and θ is the angle between the wind and the current, negative angles indicating a current direction rotated clockwise from the wind direction. These equations relate the wind-driven velocity (u, v) (in m s^{-1}) to the wind velocity (u_w, v_w) (in m s^{-1}) or the wind stress (τ_x, τ_y) (in N m^{-2}) assuming a linear relationship between the wind stress and the wind-driven current. Variables β and θ are obtained by minimizing the least square error of the model using linear least squares techniques.

The Ekman model is based upon the Ekman balance

$$if(u + iv) = \frac{1}{\rho} \frac{\partial}{\partial z} (\tau_x + i\tau_y), \quad (4)$$

where ρ is the density of water. Combining Eq. (4) with Eq. (3) and assuming that the Ekman stress is constant over the upper ocean implies a complex-valued mixing depth h :

$$h = \frac{e^{-i\theta}}{i\rho\beta f}. \quad (5)$$

After removing the wind-driven part of the velocity, we are left with the geostrophic velocity components

and ageostrophic components. Matear (1993) found that the velocities in this region are in geostrophic balance, which means that the ageostrophic contributions are small. D'Asaro et al. (1995) found that the flow is geostrophic and nearly nondivergent.

a. STORMS 87

The average β is $0.3 (\pm 0.1) \text{ m s}^{-1} \text{ Pa}^{-1}$ and the average direction θ is $-56.4^\circ (\pm 0.8^\circ)$, indicating a current to the right of the wind stress vector, as expected from the Ekman theory of wind-driven currents. The model explains 13% of the variance. The mixing depth h is found to be $|h| = 33 \pm 25 \text{ m}$ in the direction of 033.6° . The second row in Table 2 shows the statistics for the wind model corrected low-frequency velocity dataset for the STORMS 87.

Figure 5 shows that the currents have rotated toward the wind vector and that currents (dark solid line) in boxes 2 and 5 are smaller than the currents in the other boxes. The currents in box 6 are more northeastward, following the coast.

b. HEAVY 89

The average β is $0.3 (\pm 0.1) \text{ m s}^{-1} \text{ Pa}^{-1}$ and the average angle θ is $-61.8^\circ (\pm 0.6^\circ)$, indicating that the currents are on the average 61.8° to the right of the wind vector, in accordance with the Ekman theory. The model explains 27% of the variance. In this case, $|h| = 33 \pm 25 \text{ m}$ in a direction of 028.2° .

Table 3 shows the mean velocity \bar{u}, \bar{v} components, their variance, and mean and eddy kinetic energy for the HEAVY 89 dataset after subtracting the wind-driven currents. The average east–west current is reduced from 7.0 to 4.5 cm s^{-1} , while the north–south velocity changes from -1.3 to 0.1 cm s^{-1} and is not significantly different from zero. The east–west variance is smaller, while the north–south variance has increased.

Figure 6 shows that the most noticeable difference is in regions 2 and 5 in which the uncorrected currents were in a southeastward direction. After subtracting the wind-driven flow, they now are eastward, indicating that the anomalous winds were responsible for the currents running southeastward. The currents in the western boxes 1 and 4 are again stronger than in the boxes 2 and 5. While the currents in STORMS 87 and in most of the HEAVY 89 boxes turned to align closer to the wind, the currents in boxes 1 and 4 do not seem to rotate significantly.

6. Average speed

Because the drifter tracks appeared to be more contorted in STORMS 87 than in HEAVY 89, we thought it interesting to compute the actual speed of the drifters while moving through the eddies. Table 4 displays the average speed. One notes immediately that the average

TABLE 4. STORMS 87 and HEAVY 89 average speed and variance for slip and Ekman corrected currents.

| Region | STORMS 87 | | HEAVY 89 | |
|--------|--------------------------------------|--|--------------------------------------|--|
| | $ \mathbf{u} $ (cm s ⁻¹) | $ \mathbf{u} '^2$ (cm ² s ⁻²) | $ \mathbf{u} $ (cm s ⁻¹) | $ \mathbf{u} '^2$ (cm ² s ⁻²) |
| 1 | 6.6 ± 1.4 | 18.5 | 6.4 ± 1.1 | 11.9 |
| 2 | 6.1 ± 0.5 | 13.9 | 5.9 ± 0.7 | 8.3 |
| 3 | 7.1 ± 0.9 | 17.5 | 6.1 ± 0.8 | 9.5 |
| 4 | 7.0 ± 0.8 | 20.6 | 8.3 ± 0.8 | 11.1 |
| 5 | 7.5 ± 0.6 | 19.2 | 5.5 ± 0.7 | 6.6 |
| 6 | 8.1 ± 0.8 | 15.1 | 6.8 ± 1.2 | 11.6 |
| All | 7.0 ± 0.3 | 17.6 | 6.5 ± 0.4 | 10.6 |

speed $|\mathbf{u}|$ for the STORMS 87 and the HEAVY 89 regions are the same within the error bounds. This indicates that while the average speed of the drifters is the same in the two experiments, the presence of many eddies during the 1987 STORMS 87 experiment decreases the effective east–west velocity component of the drifters as they spend more time in the eddy field. This has some interesting implications for the use of drifters as well as moorings to obtain mean current estimates in regions with great variability of eddy activity.

7. Summary and conclusions

We have measured the mean circulation in a region in the northeast Pacific using mixed layer drifters and, after correcting for wind slippage, have shown that the mean velocity varies considerably between 1987 and 1989. In 1987 the mean \bar{u} , \bar{v} velocity was (3.3 ± 0.5, 0.4 ± 0.5) and in 1989 it was (6.6 ± 0.5, -1.3 ± 0.6) (in cm s⁻¹). The east–west component in 1989 is twice the 1987 component. The north–south component is statistically not different from zero in 1987 and has a southward direction in 1989. Note that in 1989, for regions 2 and 5 there is a flow in southeastward direction (Figs. 1 and 6). This is caused mainly by the winds that tended to be more eastward than northeastward. After correcting for the Ekman velocity the mean velocity becomes eastward (Fig. 6). The winds in 1989 tend to be stronger and more variable than in 1987 (Figs. 5 and 6, dashed lines). The winds also decrease in strength and increase in variability when approaching the coast (regions 3 and 6).

After removing the wind-driven Ekman velocities by matching an Ekman-type model to the observed data, the differences in mean u , v velocity increased. In 1987 the Ekman corrected velocity was (0.9 ± 0.4, 0.7 ± 0.4) and in 1989 it was (3.8 ± 0.5, 0.3 ± 0.5) (in cm s⁻¹). The east–west component in 1989 is four times larger than in 1987. The north–south component in 1987 is northward and in 1989 not different from zero. There are two obvious differences between the 1987 and 1989 dataset: 1) the temporal coverage and 2) the eddy activity.

The 1989 data tend to be on the average 10 weeks

ahead of the 1987 data and have a smaller temporal extent. This means that “anomalous” conditions will not be averaged out to the same extent as in 1987. The slip correction and the Ekman model, however, correct for anomalous wind events, reducing the relevance of the differences in temporal coverage between the two years.

Corrected for Ekman velocity, the 1987 eddy kinetic energy (EKE = 32.6 cm² s⁻²) is 30–40 times greater than the mean kinetic energy (MKE = 0.7 cm² s⁻²). In 1989 the eddy kinetic energy (EKE = 19.2 cm² s⁻²) is 2–3 times the mean kinetic energy (MKE = 7.4 cm² s⁻²). So not only is the mean kinetic energy in 1989 ten times the 1989 value, but also the eddy kinetic energy in 1989 is smaller than in 1987. Our findings support that this area has low eddy and mean kinetic energy with eddy kinetic energy being much larger than the mean kinetic energy. The data also show that eddy kinetic energy can vary greatly over time.

We decided to look at the average speed of the drifters and found that within the error bounds, the 1987 and 1989 mean speed was identical (6.7 ± 0.3 cm s⁻¹). These speeds are lower than those found by McNally (1981). Their drifters, however, had drag area ratios that were significantly smaller and therefore the wind slippage is larger (Niiler et al. 1995). Since the mean speeds are the same in the two experiments, it is unlikely that the differences in mean velocity are related to the differences in temporal coverage and it is more likely that they are related to the increased eddy activity. This is easily explained as follows: when the drifters move through a field of eddies that distorts their, generally eastward, trajectories in an up–down motion, the drifters spend more time going up and down than traveling east, reducing the mean east–west velocity estimates. One can only speculate about the cause of the increased eddy activity in the 1987 experiment when compared to the 1989 experiment. The study area is close to the frontal region between the North Pacific subtropical gyre and the Alaskan subarctic gyre and any north–south excursions of this frontal region could affect the eddy activity. Figure 1 shows drifters going north in the Alaskan Current in 1987, while Fig. 2 shows only one of the drifters going north in 1989 when approaching the coast. Most of the drifters in 1989 end up going south.

We have shown in a region in the northeastern Pacific, between the Alaskan subarctic gyre and the North Pacific subtropical gyre, that significant variability in eddy activity affects the estimates of mean velocity obtained using drifters (or moorings). This complicates obtaining reliable estimates of mean currents in areas with large variabilities in eddy activity. The possibility that the differences in velocity are caused by the differences in temporal coverage in the two years is contradicted by the estimates of mean speed that are identical within their error bounds. The conclusion is that the presence of eddies distorted the mainly geostrophic flow to move

upward/downward, reducing the eastward mean velocity.

Acknowledgments. The authors thank P. J. Stabeno for her contributions and corrections to this paper, J. Paduan for the datasets, and D. L. Williams for his suggestions and corrections to the paper. FMAJ

REFERENCES

- D'Asaro, E. A., C. C. Eriksen, M. D. Levine, P. P. Niiler, C. A. Paulson, and P. van Meurs, 1995: Upper-ocean inertial currents forced by a strong storm. Part I: Data and comparison with linear theory. *J. Phys. Oceanogr.*, **25**, 2909–2936.
- Kirwan, A., G. J. McNally, E. Reyna, and W. J. Merrell, 1978: The near-surface circulation of the eastern North Pacific. *J. Phys. Oceanogr.*, **8**, 937–945.
- Matear, R. J., 1993: Circulation within the Ocean Storms area located in the northeast Pacific Ocean determined by inverse methods. *J. Phys. Oceanogr.*, **23**, 648–658.
- McNally, G. J., 1981: Satellite-tracked drift buoy observations of the near-surface flow in the eastern mid-latitude North Pacific. *J. Geophys. Res.*, **86** (C9), 8022–8030.
- , and W. B. White, 1985: Wind-driven flow in the mixed layer observed by drifting buoys during autumn–winter in the mid-latitude North Pacific. *J. Phys. Oceanogr.*, **15**, 684–694.
- Meehl, G. A., 1982: Characteristics of surface flow inferred from a global ocean current data set. *J. Phys. Oceanogr.*, **12**, 528–555.
- Niiler, P. P., and J. D. Paduan, 1995: Wind driven motions in the northeast Pacific as measured by Lagrangian drifters. *J. Phys. Oceanogr.*, **25**, 2819–2830.
- , A. S. Sybrandy, K. Bi, P. M. Poulain, and D. Bitterman, 1995: Measurements of the water-following capability of Holey-sock and TRISTAR drifters. *Deep-Sea Res.*, **42** (11/12), 1951–1964.
- Paduan, J. D., and P. P. Niiler, 1993: The structure of velocity and temperature in the northeast Pacific as measured with Lagrangian drifters in fall 1987. *J. Phys. Oceanogr.*, **23**, 585–600.
- Reid, J. L., and R. S. Arthur, 1975: Interpretation of maps of geopotential anomaly for the deep Pacific Ocean. *J. Mar. Res.*, **33**(Suppl.), 37–52.
- Sverdrup, H. W., M. W. Johnson, and R. H. Fleming, 1942: *Oceans, Their Physics, Chemistry, and General Biology*. Prentice-Hall, 1087 pp.
- Tabata, S., 1965: Variability of oceanographic conditions of Ocean Station P in the northeast Pacific Ocean. *Trans. Roy. Soc. Can.*, **3**, 367–418.
- Wakata, Y., and Y. Sugimori, 1990: Lagrangian motions and global density distributions of floating matter in the ocean simulated using shipdrift data. *J. Phys. Oceanogr.*, **20**, 125–138.
- Wyrtki, K., 1975: Fluctuations of the dynamic topography in the Pacific Ocean. *J. Phys. Oceanogr.*, **5**, 450–459.